Fermi Surface in Gallium Determined from the Radio-Frequency Size Effect*

AKIRA FUKUMOTO AND M. W. P. STRANDBERG
Department of Physics and Research Laboratory of Electronics, Massachusetts Institute of Technology, Cambridge, Massachusetts

(Received 15 August 1966)

The extremal cross sections of the Fermi surface (FS) in a gallium single crystal were measured by using the radio-frequency size effect (RFSE), with rf frequencies of 2–8 MHz. The single crystal was grown in a shape of a plate with thickness ≈ 0.2 mm, and its crystal axis was verified within one degree of arc. The derivative of the real part of the surface impedance of the plate with respect to the magnetic field was measured, and the RFSE signals of various line shapes were observed for magnetic fields below 500 G. An interpretation of these line shapes is given. The results of the experiment are compared with the FS predicted from calculations using an augmented-plane-wave (APW) expansion for the wave functions carried out by Wood and with the results of several other experimental methods. The comparisons show that the APW predictions for $E_F = 0.400$ Ry are quite accurate for some bands. The APW band 7 is verified in three orthogonal planes with an accuracy better than 30%. The APW band 5 is verified in two orthogonal planes, and the deviation is less than 25%. The APW band 8 is verified in a plane with an accuracy of better than 10%. The existence of the APW band 6 is strongly indicated in two orthogonal planes, and its topology is suggested by the experiment.

I. INTRODUCTION

THE Fermi surface (FS) in gallium has been calculated by Reed and Marcus[1] and also by Slater, Koster, and Wood[2], from band energies calculated by using orthogonalized plane waves (OPW) as wave functions, and the complex topology of the FS has been shown. The experimental information then available,[1,3–5] showed that the calculations using an OPW expansion were a crude approximation and did not generally explain the experimental results adequately. Wood[6] has calculated the FS, using the augmented-plane-wave method (APW), and several early reports[5–9] have indicated better agreement with experimental data. Results have been reported for experiments on gallium magnetoresistance,[1,4,10] ultrasonic attenuation (UA),[5,7,8,11] the de Haas–van Alphen effect (dHuA),[3,9] and, most recently, on the size effect. The radio-frequency size effect (RFSE) was first reported by J. F. Gantmakher[12] in his study of FS of tin. His succeeding paper showed the very good agreement between the experimental data obtained with this method and theoretical predictions.[13] The RFSE was first applied to the study of FS in gallium by Sparlin and Schreiber,[14] and later by Cochran and Shiffman,[15] and P. H. Haberland.[16] The results of the first study, as Wood pointed out, are much too complicated for simple interpretation and the data do not have the symmetry required by theory; therefore, comparison with theory cannot be readily made. More detailed experiments were necessary for a valid appraisal of the APW calculation. Early in the research work reported here, the FS of gallium was studied by using UA at microwave frequencies,[8] and some of the results showed good agreement with the APW predictions. Later, experiments were carried out to compare the results of RFSE[17,18] and UA experiments, to obtain a more precise description of the actual FS. We note that UA and RFSE are similar in their experimental techniques in that they both use a form of geometric resonance in the metals. The results of these two experiments, therefore, should be very similar. As we shall show, this turned out to be true in our experiments.

In Sec. II, we shall discuss the theoretical basis for understanding the RFSE experimental results. The experimental apparatus will be described in Sec. III. Sample preparation will be discussed in Sec. IV. The

* This work was supported by the Joint Services Electronics Program under Contract No. DA36-039-AMC-03200(E).

[1] W. A. Reed and J. A. Marcus, Phys. Rev. **126**, 1298 (1962).
[2] J. C. Slater, G. F. Koster, and J. H. Wood, Phys. Rev. **126**, 1307 (1962).
[3] D. Shoenberg, Trans. Roy. Soc. (London) **A245**, 1 (1952).
[4] J. Yahia and J. A. Marcus, Phys. Rev. **113**, 137 (1959).
[5] B. W. Roberts, Phys. Rev. Letters **6**, 453 (1961).
[6] J. H. Wood, Phys. Rev. **146**, 432 (1966).
[7] P. A. Bezuglyi, A. A. Galkin, and S. E. Zhivago, Zh. Eksperim. i Teor. Fiz. **47**, 825 (1964) [English transl.: Soviet Phys.—JETP **20**, 552 (1965)].
[8] A. Fukumoto, Quarterly Progress Report No. 78, Research Laboratory of Electronics, MIT, Cambridge, Massachusetts, 1965, p. 15 (unpublished).
[9] A. Goldstein and S. Foner, Phys. Rev. **146**, 442 (1966).
[10] W. A. Reed and J. A. Marcus, Phys. Rev. **130**, 957 (1963).
[11] N. Tepley, Ph.D. thesis, Department of Physics, MIT, 1963 (unpublished).
[12] V. F. Gantmakher, Zh. Eksperim. i Teor. Fiz. **43**, 345 (1962) [English transl.: Soviet Phys.—JETP **16**, 247 (1963)].
[13] V. F. Gantmakher, Zh. Eksperim. i Teor. Fiz. **43**, 345 (1962) [English transl.: Soviet Phys.—JETP **17**, 549 (1963)].
[14] D. M. Sparlin and D. S. Schreiber, in *Proceedings of the Ninth International Conference of Low-Temperature Physics, Columbus, Ohio, 1964*, edited by J. G. Daunt, D. V. Edwards, F. J. Milford, and M. Yaqub (Plenum Press, Inc., New York, 1965), p. 823.
[15] J. F. Cochran and C. A. Shiffman, Phys. Rev. **140**, A1678 (1965).
[16] P. H. Haberland, M.S. thesis, Department of Physics, MIT, 1966 (unpublished).
[17] A. Fukumoto, Quarterly Progress Report No. 79, Research Laboratory of Electronics, MIT, Cambridge, Massachusetts, 1965, p. 14 (unpublished).
[18] A. Fukumoto, Quarterly Progress Report No. 81, Research Laboratory of Electronics, MIT, Cambridge, Massachusetts, 1966, p. 8 (unpublished).

experimental results will be presented and discussed in Sec. V.

II. THEORY

When a metal plate is placed in a magnetic field whose direction is parallel to the surface of the plate, the electrons in the metal rotate in a plane perpendicular to the field direction. If the field is so chosen that the orbit radii of the electrons exactly fit between the sample faces, the surface impedance of the metal Z shows a singularity at this value of magnetic field H_0 as the field is varied in magnitude. This behavior of Z may be understood heuristically by noting that when the field is smaller than H_0, all of the electrons are scattered at the crystal surfaces and hence their contribution to the metal conductivity is reduced. On the other hand, when the field is larger than H_0, part of the electrons complete the full rotation and contribute more strongly to the conductivity at the surface of the crystal. The critical value of the magnetic field H_0 is determined from the integration of the equation of motion of the electron for one-half the period of rotation of the electron in magnetic field $\mathbf{H}$.

$$\hbar\int\frac{d\mathbf{k}}{dt}dt=\int\frac{e}{c}(\mathbf{v}\times\mathbf{H})dt, \tag{1}$$

$$\Delta\mathbf{k}=(e/ch)\Delta\mathbf{r}\times\mathbf{H}, \tag{2}$$

where $\mathbf{k}$ is the wave vector of the electron, e is the electronic charge, $\mathbf{v}$ is the velocity of the electron, r is the position vector of the electron, and Δ indicates the variation of the parameter in one-half of a period of rotation. With the magnetic field direction parallel to the surface of the sample, RFSE resonance occurs when $|\Delta\mathbf{r}|=d$, where d is the thickness of the sample.

The FS has a center of inversion symmetry at the center of the Brillouin zone, and since $|\Delta\mathbf{k}|=2|\mathbf{k}_F|$, Eq. (2) may be written

$$|\mathbf{k}_F|=\tfrac{1}{2}H_0ed/ch. \tag{3}$$

The electron wave vector has been restricted to a wave vector at the Fermi surface of the metal, $\mathbf{k}_F$, since only those at, or near, the Fermi surface can absorb energy from the electric field imposed on the surface. In general, the number of electrons satisfying the resonance condition, $|\Delta\mathbf{r}|=d$, for a given value of the magnetic field H_0 will be vanishingly small, and only at or near extremal orbits on the Fermi surface will the number of electrons that approximately satisfy this condition for a small variation of $\mathbf{k}_F$ be sufficiently great to have a measurable effect on the surface conductivity.

The surface impedance of the sample can be found from Maxwell's equation as follows[19]: Choose a coordinate system (Fig. 1) whose oy axis is parallel to the surface of the sample, whose oz axis is parallel to the magnetic field direction, and whose ox axis lies in a plane through $\mathbf{H}$ and the internal normal to the metal surface $o\xi$.

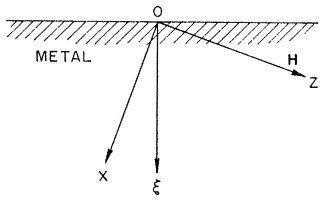

FIG. 1. Coordinate system for the metal plate. Electric field applied at $\xi=0$.

The high-frequency electric field $\mathbf{E}$ in the y direction satisfies Maxwell's equation:

$$\frac{d^2E(\xi)}{d\xi^2}=\frac{4\pi i\omega}{c^2}J(\xi), \tag{4}$$

where $J(\xi)$ is the current density along the y direction and is related to the distribution function of the electrons.

If $J(\xi)$ and $E(\xi)$ are continued with even symmetry into the region $\xi<0$, that is, if it is assumed that $E(-\xi)=E(\xi)$ and also that $E(\xi)=0$ for $|\xi|>d$, the Fourier components of the field $\mathcal{E}(\kappa)$ obey the equation

$$-|\kappa|^2\mathcal{E}(\kappa)-2E'(0)+2E(d)|\kappa|\sin|\kappa|d+2E'(d)\cos|\kappa|d=4\pi i\omega\sigma(\kappa)/c^2\mathcal{E}(\kappa), \tag{5}$$

where $\sigma(\kappa)$ is a component of the conductivity tensor for the electric field component having a wave vector κ. The continuity of the electric field strength and its derivative at the boundary require that the fourth term in Eq. (5) be much smaller than the third term. If the metal is placed in a high-frequency electric field that is impressed antisymmetrically on both surfaces of the sample (the usual experimental condition), the following relationships hold:

$$E(0)=-E(d),\quad E'(0)=-E'(d). \tag{6}$$

In this case, Eq. (5) becomes

$$\mathcal{E}(\kappa)=-\frac{2}{\kappa^2+4\pi i\omega\sigma(\kappa)/c^2}[E'(0)+E(0)|\kappa|\sin|\kappa|d]. \tag{7}$$

If the thickness of the sample is infinitely large, then the third and fourth terms on the left-hand side of (5) vanish, and we obtain

$$E(0)=-\frac{2}{\pi}\int_0^\infty\frac{E'(0)}{\kappa^2+4\pi i\omega\sigma(\kappa)/c^2}d|\kappa|. \tag{8}$$

As an approximation, (8) may be used in (7) to obtain the surface impedance Z defined by

$$Z=-(4\pi i\omega/c^2)E(0)/E'(0) \tag{9}$$

[19] E. A. Kaner, Zh. Eksperim. i Teor. Fiz. 44, 1036 (1963) [English transl.: Soviet Phys.—JETP 17, 700 (1963)].

as follows:

$$Z(\beta)=\frac{8i\omega D}{c^2}I(0)\left[1+\frac{2}{\pi}\frac{dI(\beta)}{d\beta}\right], \tag{10}$$

where

$$I(\beta)=\frac{1}{D}\int_0^\infty \frac{\cos|\kappa|d}{\kappa^2+4\pi i\omega\sigma(\kappa)/c^2}d|\kappa|,$$

$$D=2\hbar|\mathbf{k}|c/eH \quad \text{(diameter of the electronic orbit)}, \tag{11}$$

$$\beta=d/D.$$

Equation (10) can be rewritten

$$\frac{Z-Z_\infty}{Z_\infty}=\frac{2}{\pi}\frac{dI(\beta)}{d\beta}, \tag{12}$$

where Z_∞ is the surface impedance of a semi-infinite metal slab. Generally speaking, Z_∞ is a slowly varying function of the magnetic field,[19] and the contribution to the singularity of Z comes from $dI(\beta)/d\beta$. Since the function $I(\beta)/I(0)$, which is proportional to $E_\infty(d)/E_\infty(0)$, describes the electric field distribution at a distance d from the surface of the sample when it is semi-infinitely large, if $E_\infty(d)/E_\infty(0)$ is known, the function $(Z-Z_\infty)/Z_\infty$ may be determined. Hence the line shape of the signal obtained from the RFSE resonance may be determined. The function $I(\beta)/I(0)$ has been studied by Kaner[19] for particular orientations of the magnetic field and for particular values of the mean-free path of the electrons. For example, the field distribution schematically represented by Fig. 2 (a) produces $(Z-Z_\infty)/Z_\infty$, as shown in Fig. 2(b).

The linewidth of the surface impedance signal is determined by the width of the spikes of $I(\beta)$, and the width of these spikes is determined by the electromagnetic penetration into the sample (i.e., the skin depth) and the spread in the wave vectors of the electrons that contribute appreciably to the surface conductivity. When the mean free path of the electrons is large compared with the skin depth δ, the skin depth has anomalous properties. As the frequency of the rf current is varied, however, a qualitative change in the width of $I(\beta)$ occurs and, as a consequence, the various identifiable portions of the signal line occur at varying mag-

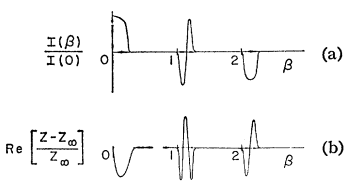

FIG. 2. Example of the field distribution function $I(\beta)/I(0)$. The normalized magnetic field is β, Z is the surface impedance of a finite sample when it is excited antisymmetrically, and Z_∞ is the surface impedance of a semi-infinite sample.

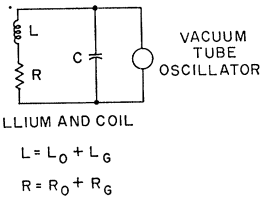

FIG. 3. Equivalent circuit for gallium and coil in vacuum-tube oscillator ($L=L_0+L_G$, $R=R_0+R_G$).

netic field values as this frequency is changed.[20] This narrowing of the signal wave form as the rf frequency is increased is a result of a decrease in penetration of the rf electric field; hence, there is a decrease in the indeterminancy of the diameter of the electron orbit required for RFSE resonance. The portion of the signal line shape which shifts most slowly with respect to magnetic field when the rf frequency is varied may thus be identified as arising from electrons with orbit diameters equal to that of the sample thickness. This means that, for a single line, the inflection point of the signal that occurs at the lowest field should be used to determine the critical magnetic field, or β. For overlapping lines the inflection points will be obscured, but the points on the curve which move most slowly with frequency may be used to determine the critical magnetic fields.[21]

III. APPARATUS

In the experiments reported here, the real part of the surface impedance was measured. The measurements were made by detecting the change of the high-frequency voltage of a coil that was wound around the gallium plate. The equivalent circuit of the coil with the gallium sample may be drawn as shown in Fig. 3. The values of L_G and R_G correspond to the inductance and resistance of the coil caused by the electrons in gallium, that is, the reaction to, and the absorption of, the rf field. L_0 and R_0 represent the residual inductance and dc resistance of the coil. The values R_G and L_G are related to the surface impedance of the plate by the following relations:

$$R_G=n^2S\,\mathrm{Re}(Z), \quad L_G=(2cs/\omega)\mathrm{Im}(Z), \tag{13}$$

where n is the number of turns per unit length, s is the length, and S is the total area of the coil. The change of the output voltage ΔV of the oscillator is given approximately by

$$\Delta V=\frac{1}{2}\left(\frac{A_1+G}{-A_3}\right)^{-1/2}\frac{C}{L}\Delta R_G, \tag{14}$$

where A_1 and A_3 are real constants that depend on the characteristic curve of the vacuum tube, and G is the steady-state conductance in the resonant circuit

$$G=CR/L. \tag{15}$$

[20] A. Fukumoto and M. W. P. Strandberg, Phys. Letters 23, 200 (1966).

[21] A. Fukumoto, Ph.D. thesis, Department of Physics, MIT, 1966 (unpublished).

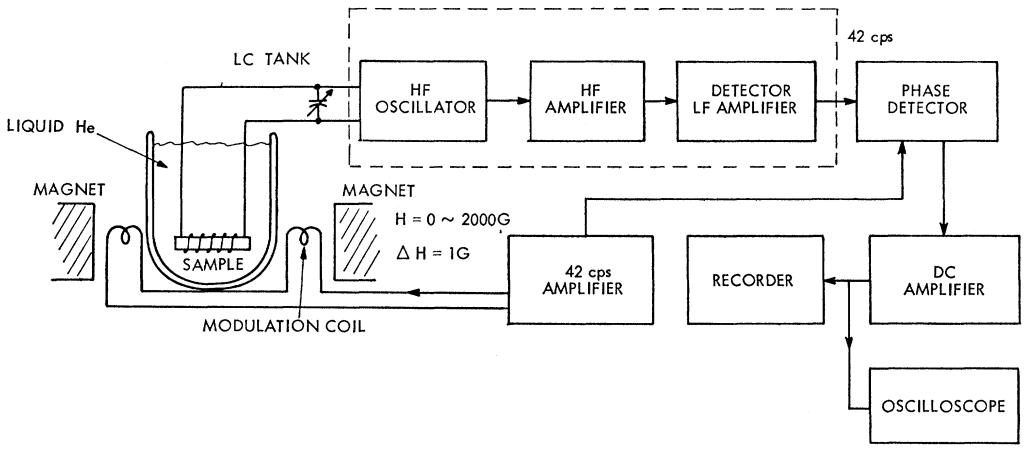

FIG. 4. Experimental arrangement for RFSE.

The change in the oscillator voltage is proportional to the change in the real part of the surface impedance as given by Eqs. (13) and (14).

The output voltage of the oscillator was amplified and detected by a crystal diode, and the low-frequency component was amplified and demodulated in a phase detector. The block diagram of the system is given in Fig. 4. This system is essentially identical to the usual NMR marginal oscillator detector. As usual, the static magnetic field was modulated at a low frequency and the derivative of the real part of the surface impedance, $d\,\mathrm{Re}(Z)/dH$, was measured. The modulation frequency was chosen as 42 Hz, for which frequency the skin depth in gallium is large enough to allow penetration of the modulation field into the gallium sample. The sample was fixed on a nylon disk that could rotate through 360° of arc in two orthogonal planes; the angles could be measured to 0.2°. The direction of the static magnetic field was chosen to be parallel to the surface of the sample. The parallelism of the field with the sample face was determined by observing the signal line shapes as the sample face was rotated with respect to the magnetic field. Similar signals occur in this sequence of rotation in pairs, and these pairs are used to determine the angle for which the sample face is parallel to the static magnetic field. The sample and the nylon disk were fixed on a stainless-steel holder and placed directly in the liquid-helium bath which was held in a conventional double Dewar system. The magnetic field was applied from outside the Dewar. The separation of the poles of the magnet was 3 in. and the pole diameter was 11 in.

The frequency of the marginal rf oscillator was varied between 2 and 8 MHz because, for this range of frequencies, the skin depth δ of gallium satisfies the conditions for RFSE resonance:

$$\delta/d \ll 1 \tag{16}$$

and

$$\omega \ll \omega_c, \tag{17}$$

where ω is the radian frequency of the oscillator, and ω_c is the radian cyclotron frequency of the electron.

IV. FABRICATION OF SAMPLES

Gallium has a melting point at 29.78°C. When it solidifies, its volume increases approximately 0.3%. When it is pure, it supercools very easily. These characteristics were used to fabricate the samples. The sample's thickness in most cases was chosen to be approximately 0.2 mm which distance corresponds to an RFSE resonant magnetic field for gallium of less than 500 G. A gallium single crystal of such thickness and an area of 1.3 cm×1.3 cm was grown between two Lucite molds. The gallium ingot had a purity of 99.9999% as purchased from the United Mineral and Chemical Corporation in New York City. The ingot was heated in a very clean beaker with a hot-water bath. The melted gallium was drawn into a syringe and very carefully injected into the Lucite molds. The molds were placed on a crystal-growing apparatus that was composed of a base, a support, and a goniometer holding

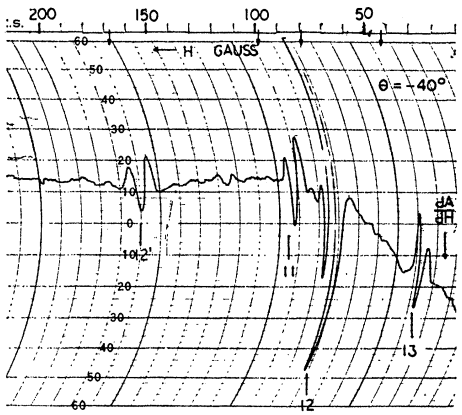

FIG. 5. Recording of the derivative of the absorbed power with respect to the magnetic field dA/dH versus magnetic field H for RFSE (c crystal, $\theta = -40°$, $T = 4.2$°K). The arrows indicate the appropriate values of H_0.

a seed crystal that could be aligned with respect to the axes of the mold. The melted gallium in the mold was kept supercooled at a temperature of approximately 20°C. The seed crystal of known orientation was then carefully lowered into contact with the bead protruding from the mold of the supercooled gallium. The crystallization began immediately after contact. The system was left undisturbed for 20 min, at which time the crystallization was complete. A sample made in this way has mirror surfaces, and the deviation of its thickness from the mean is usually less than 1%. With seed crystals of three orthogonal orientations properly positioned by rotation of the goniometer axes, crystals of any orientation can be grown. The orientation of the crystal axes was checked by a back-reflection Laue picture, and only those samples whose orientations were defined by the flat surface within 1° were used for our experiments.[22]

V. RESULTS AND DISCUSSION

A recording of the derivative with respect to magnetic field of the absorbed power versus the magnetic field (dA/dH versus H) of the RFSE is given in Fig. 5. This is a recording for a crystal whose normal to the broadface is parallel to the c axis of the crystal. We shall call this a c crystal with similar meaning to the terms a crystal and b crystal. In the recording shown in Fig. 5, the angle θ between the magnetic field and the a axis of the crystal was $\theta=-40°$, and the temperature of the bath T was 4.2°K. The magnetic field modulation amplitude was $\Delta H=1$ G peak-to-peak. Four signals appear in this figure. The numbers below the signals correspond to the numbers of the Fermi-surface curves given in Fig. 6. The line 12′ is the second harmonic of line 12, and occurs when the electron orbit diameter is half the thickness of the crystal. There is something to be learned about the properties of electrons in gallium such as the wave-vector dependence of the mean free paths from a study of these second-harmonic signals, but this study is not the subject of the present paper and so these signals will not be discussed at length.

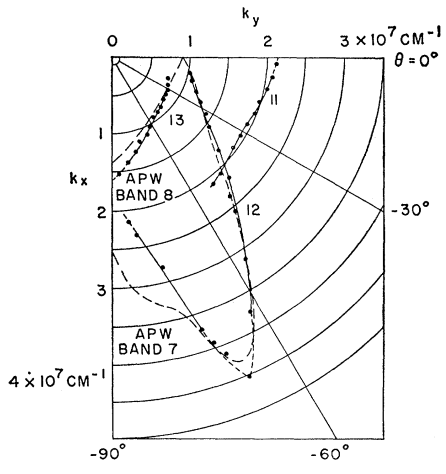

FIG. 6. Extremal wave vectors in k_x-k_y plane obtained from RFSE experiments and APW predictions for bands 7 and 8. Numbers of curves correspond to those in Fig. 5. Long broken lines are predictions from APW calculations.

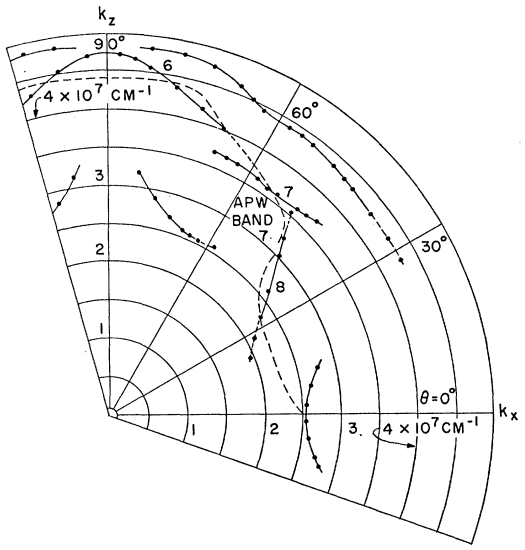

FIG. 7. Extremal wave vectors in k_x-k_z plane obtained from RFSE and APW predictions for band 7.

The magnitude of the wave vector corresponding to the extremal portion of the Fermi surface of gallium is found from Eq. (3), for a single line, using the inflection point occurring at the lowest magnetic field to determine H_0, since d is known. Since the direction of this vector is perpendicular both to the direction of the magnetic field and the normal to the sample plate, a cross section of the Fermi surface may be obtained by rotating the direction of the magnetic field in the broadface of the crystal. Figure 6 shows a cross section of the Fermi surface so obtained with the same crystal that was used for Fig. 5 (c crystal).

The solid line and the short broken line in Fig. 6 indicate the experimental curve as determined by the small circles corresponding to experimental points. The signals were as strong as that shown in Fig. 5. except at the portion indicated by the short broken lines in Fig. 6, where the signal became weak. The long broken lines are the APW predictions as calculated by Wood[6] for $E_F=0.400$ Ry. The experimental data agree very well with the data obtained from the ultrasonic attenuation geometric resonance measurements of Bezuglyi, Galkin, and Zhivago (BGZ)[7] at 200 MHz, and by the present authors[8] at 900 MHz. The comparison with the APW prediction, as pointed out by Wood in discussing the data of BGZ, shows that band 8 (curve 13 in Fig. 6) which is the so-called "cigar" band, agrees almost perfectly with the experimental result. The wing-shaped

[22] We are indebted to W. D. Gregory and P. H. Haberland for help in setting up the crystal-growing apparatus.

curve 12 also agrees very well with the APW prediction for band 7. This part of the band 7 is the so-called "butterfly." The agreement at the wings of the butterfly is almost perfect, and only at the head is there a difference of approximately 30%. In this case, the APW prediction for $E_F=0.410$ Ry gives much too large a surface, and the fit becomes even poorer.

Curve 11 appears for extremal wave vectors $\sim 60°$ from the k_y axis, and we tend to interpret this as APW band 5; the deviation from prediction in this case is $\sim 25\%$. The curve disappears at $\theta=-60°$ because the small opening of this band at $k_x=\pi/a$ on this surface makes a smooth continuation of the extremal orbit impossible.

In Figs. 7 and 8, the wave vectors in the (k_x-k_z) plane are shown. The crystal in this case has the normal to the plate parallel to the b axis. There are six different curves. They are numbered 5–10. The signals corresponding to these curves are very strong, except at the directions subtended by small dashed lines. In Fig. 7, curves 6, 7, and 8 are compared with APW predictions for band 7. The fit is very good, except at a small angular range near the k_x axis where the line disappears. The disappearance may be understood as follows. The electrons that give rise to signals that would continue curve 8 to the k_x axis have their orbits through the butterfly wing. This means that the radii of curvatures of this surface are small and only a few electrons contribute to the signal. Apparently, the number is too small to be detectable with our apparatus. If the extension of curve 8 were measurable, the curve would cross the

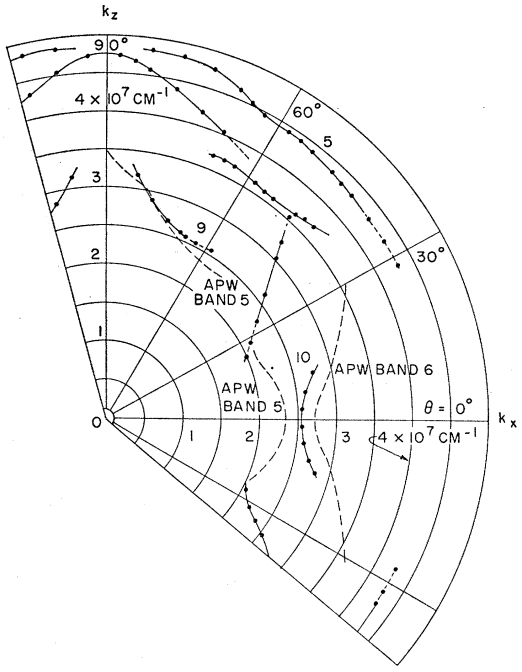

FIG. 8. Extremal wave vectors in k_x-k_z plane obtained from RFSE and APW predictions for bands 5 and 6.

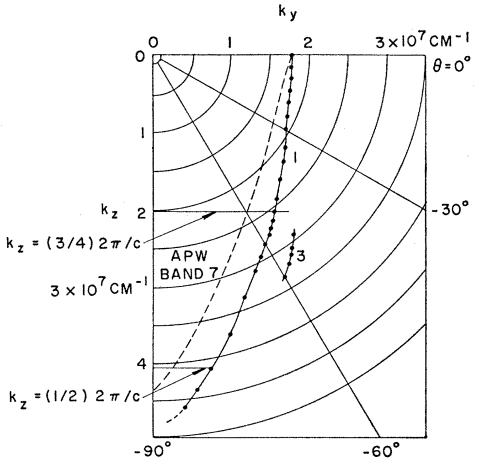

FIG. 9. Extremal wave vectors in k_y-k_z plane obtained from RFSE and APW predictions for band 7.

k_x axis at 2×10^7 cm^{-1}. We know this from the c-axis data (Fig. 6).

Curve 7 appears only in a narrow angular range where curve 6 joins curve 8. The high degree of curvature at $\theta=48°$ would allow one surface to produce two resonances. θ in this case is the angle between the magnetic field direction and the c axis of the crystal. There is a possibility that curve 7 is a part of some other band, but we are unable to identify it. In these cases, once again, the APW predictions with $E_f=0.410$ Ry give surfaces that are too large and the fit is poorer.

Curve 9 appears for an angular range of $\theta=55°$–$90°$. This signal is very strong at angles 10°–30° from the k_z axis. From Fig. 8 we can easily identify this as the APW prediction for band 5. The fit in this angular range is perfect. The signal, however, disappears at $\theta=55°$.

Curve 10 appears for $\theta=\pm15°$, and it shows the strongest signal at the axis. Two explanations are available for curve 10. Neither is as good as the fit for curve 9. One may consider that curve 10 is part of band 5. The shape, however, is not the same as that of the APW prediction shown in Fig. 8. If curve 10 is indeed the extremal intersection of band 5, then it must connect to curve 9. This connection was not observed. The second explanation for curve 10 is that the signal arises from band 6; however, we need some alteration to the APW prediction for this explanation to fit satisfactorily. Band 6 is called by Goldstein and Foner[9] (GF) the "two-headed camel." The legs of a camel are connected to those of the other camel located at a symmetric position with respect to the center of the Brillouin zone. These connected legs and the bodies of the camels produce an open orbit along the k_x direction, which, at the present stage, is contradictory to the experimental observations. Disconnected legs would give a closed orbit that may match curve 10 of the data (see Fig. 8).

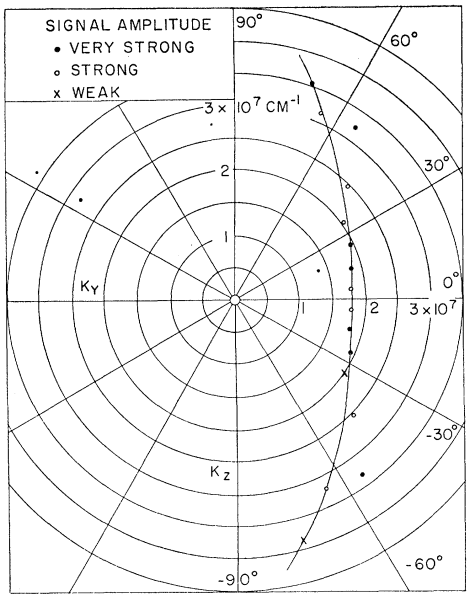

FIG. 10 Extremal wave vectors in k_y-k_z plane obtained from geometric resonance in ultrasonic attenuation at 883 MHz.

Curve 5 extends almost circularly from $\theta=90°$ to 30°. The immediate identification of this curve with APW predicted bands is not possible. We can suggest from the dimension of the curve that this surface is associated with the band-6 camel and connected to curve 10 near the k_x axis. For this to be so, however, there must be a large alteration in the band. This point will be discussed below. Figure 9 shows the wave vectors in a polar graph as determined from the RFSE data with an a axis crystal. Two curves are shown, numbered 1 and 3. These curves agree very closely with the data obtained from UA by the authors at 900 MHz and by BGZ at 200 MHz. Our UA data are given in Fig. 10. Curve 1 is derived from very strong signals for all angles, except in a very narrow angular range ($\pm5°$) near the k_z axis where the signal disappears. When the ultrasonic data were first obtained by the authors,[8] curves 1 and 3 were not recognized as being separate surfaces. Our subsequent data showed them to be. A recording of a RFSE signal at $\theta=-55°$ is given in Fig. 11, where θ is the angle between the magnetic field direction and the c axis of the crystal. The line corresponding to curve 3 appears at $\theta=-50°$ and becomes a fairly large signal at $\theta=-55°$ and disappears at $\theta=-61°$. Subsequent analysis of the RFSE line shape as a function of rf frequency also established the separation of these two surfaces.

The shape of curve 1 immediately suggested to BGZ that it be identified with the OPW band 8. The APW band 8 ("cigar") has a shape similar to the OPW band, only it is slightly shorter in the k_z direction. The identification with the APW band 8 is probably not correct. While the large axis of the cigar agrees very well with predictions, the short axis is too small in the APW prediction by a factor of 2. As we have shown, the fit of the predicted surface for bands 7 and 8 with the experimental data in the k_x-k_y and k_x-k_z planes is almost perfect. If there is some error in APW calculations, it is small and does not effect the general shape of the Fermi surface, as far as these bands are concerned. Since these bands fit so well in the other orientations that have been measured, it is not easy to understand why the predicted surface for band 8 should fit the data taken with the a crystal so poorly. From Fig. 6, we can determine the maximal orbit wave vector in the k_y direction at $k_x\simeq3.5\times10^7$ cm^{-1}. It is $\sim1.78\times10^7$ cm^{-1}. This value coincides with the short radius of curve 1 which we call "the boat" hereafter. This is not accidental. The electrons that contribute to RFSE move in orbits perpendicular to the plane of the boat. That is, the electrons' orbits are in the k_x-k_y plane. When one looks at the electrons that produce the RFSE resonance with a maximum k_y, one is looking at the electrons that are moving around the butterfly's wing shown in Fig. 12. This butterfly is 1.78×10^7 cm^{-1} wide at its longest dimension in the k_y direction (see Fig. 12). This is the value of the maximum k_y in the boat. In measuring the boat wave vectors, one starts with orbits going around the butterfly, which pass through point A in Fig. 12. As θ is increased, orbits similar to those going through point B in Fig. 12 begin to contribute to the surface impedance signal. Finally, when $\theta=90°$, orbits that go through C and the butterfly's body become the most important in giving the RFSE signal. Those orbits that pass through point C give the maximum k_z dimension of the boat. In the published APW calculation only three cross sections in the k_y-k_z plane of band 7 are shown ($k_x=\frac{1}{2}\pi/a$, $\frac{3}{4}\pi/a$, π/a). One can use the APW calculation for the k_x-k_y plane however, to pick the maxima of k_y for the extremal orbits at $k_z=\frac{1}{2}2\pi/c$, $\frac{3}{4}2\pi/c$, $2\pi/c$. These points are plotted in Fig. 9, together with the experimental

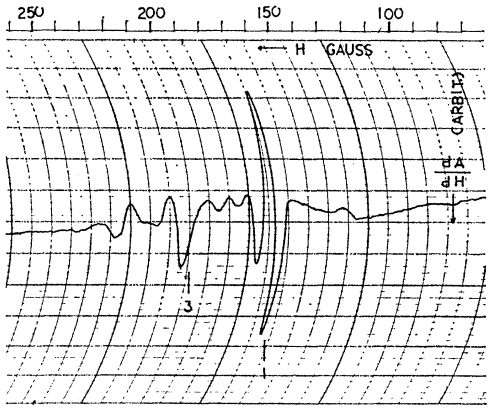

FIG. 11. Recording of the derivative of the absorbed power with respect to the magnetic field dA/dH versus magnetic field H obtained with RFSE (a crystal, $\theta=-55°$, $T=4.2°$K).

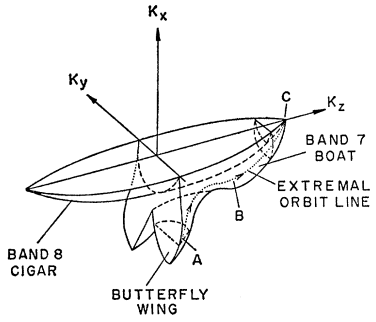

FIG. 12. The shape of band 7 (butterfly and boat) and band 8 (cigar) near the hexagonal face of the Brillouin zone.

data. It may be seen that these points are in fairly good agreement with our RFSE data. Note that the points of the boat need not be coplanar. Each point has its own k_z coordinate. The boat is actually the projection on the k_y-k_z plane of the line indicated by arrows in Fig. 12.

Curve 3, which is almost identical with BGZ's data, was suggested by Wood to represent holes in band 6. It is very likely that curve 3 is the shoulder of the camel in the APW calculation (see APW surface at $k_x=\frac{3}{4}\pi/a$). There are large differences, however, between the predicted shape of this band and the experimental data in the other two directions, and so one probably should not expect good agreement between the APW prediction and the result of RFSE measurements.

Curve 5 of Fig. 8 was identified with band 6, and it has been connected to curve 10. Although the dimension of the cross section of these curves is very close to the value suggested by the APW calculations for band 6, the shape of these curves differs from that corresponding to the largest cross section of the APW prediction for band 6, that is, in the $k_y=0$ plane.

Goldstein and Foner's data obtained by using dHvA effect gave areas of the cross section of the extremal orbits on FS. They obtained a value for the area of band 6 of 0.60 Å^{-2} (sheet XII in GF). The closed orbit corresponding to curves 5 and 10 gives the value 0.57 Å^{-2} which agrees within experimental error with the value obtained by GF. We therefore consider that curves 5 and 10 correspond to the largest cross section of band 6 as obtained with a b-orientation crystal. Also, GF give 0.56 Å^{-2} as the cross-section area for band 6 as obtained with an a-orientation crystal; however, this value is a factor of 2 too large compared with the largest cross section obtained in the APW calculation. If curve 3 is extrapolated smoothly, a cross section for band 6 with a cross-section area of approximately 0.25 Å^{-2} is obtained, which is in reasonable agreement with the APW surface. The various data[9,23,24] taken with the magnetic field lying in the bc plane suggest the existence of open orbits when the magnetic field direction is more than 13.5° away from the k_y axis. The combination of this information and that of curve 3 suggests that this band is multiply connected at angles more than 13.5° and less than 30° away from the k_z axis.

VI. CONCLUSION

Cross sections of the Fermi surface of gallium single crystal corresponding to extremal orbits of the electrons obtained with RFSE, together with data obtained with geometric resonance in ultrasonic attenuation, have been compared with APW predictions. The comparison of the present RFSE data with APW predictions shows that the APW predictions for $E_F=0.400$ Ry are quite accurate for some bands.

Band 7, butterfly and boat, is found to be extremely accurately predicted for crystals in a-, b-, and c-axis orientations. The deviation of the data from the APW predictions is, for the most part, less than 10%, and only at the butterfly's head is it as great as 30%. The signal to which the electrons in band 8 ("cigar") give rise was obtained with crystals having a c orientation, and the deviation of these data from APW predictions is less than 10%. The APW prediction for bands 5 and 6 was verified with RFSE measurements on crystals with a b-orientation, and here the deviation is less than 5%. Band-5 holes were also measured by using c-orientation crystals, and it was found that the APW prediction is narrower in the k_y direction than the experimentally determined surface by 25%.

The surface predicted for band 6 ("camel") holes in the APW calculation is quite complicated. We are sure both from the data obtained with a crystals with the RFSE experiments and from the data obtained with geometric resonance in ultrasonic attenuation experiments that there are protuberances (camel's shoulder) in the k_y-k_z plane 35° off the k_z axis, as the APW prediction postulates. The b-axis data suggest that the general shape of this band determined from RFSE experiments on b crystals is different from the APW predictions, although the area of the cross section is very close to the APW value. The data of the present experiment suggest that the shape of the band 6 surface intersection in the k_x-k_z plane is almost circular in the sector from 0°–60° away from the k_z axis, and that it has a radius$\approx 4.5\times 10^7$ cm^{-1} which rapidly decreases near the k_x axis. In all cases, the APW prediction with $E_F=0.410$ Ry showed poorer agreement with the experimentally determined surfaces than those with $E_F=0.400$ Ry.

Since both RFSE and UA techniques were used in the course of this work it may be pertinent to compare the usefulness of the two methods. Technically the RFSE method is simpler and has greater sensitivity. The UA method requires not only a single crystal but also one well bonded to piezoelectric drivers. The experimental techniques have been developed to ac-

[23] Y. Shapira and B. Lax, Phys. Rev. 138, 1191 (1965).
[24] J. Condon, Bull. Am. Phys. Soc. 9, 239 (1964).

complish this task, but the bond is readily broken and the probability of a successful experiment is thus lowered. Finally when two or more extremal orbits exist for a given crystal-field orientation the RFSE method is definitely superior since the signals are either resolved, or maybe disentangled using the frequency variation techniques described in Ref. 20. On the other hand, the UA method yields periodic signals which must be separated by analyzing the signal curves and this proves to be tedious and susceptible to large inaccuracy.

ACKNOWLEDGMENTS

The authors would like to express their gratitude to J. H. Wood for furnishing the results of his APW calculations before publication. They are indebted to R. F. Newnham for the hospitality of his x-ray laboratory and his advice in interpreting Laue photographs.

PHYSICAL REVIEW VOLUME 155, NUMBER 3 15 MARCH 1967

Piezotransmission Measurements of Phonon-Assisted Transitions in Semiconductors. I. Germanium

W. E. ENGELER, M. GARFINKEL, AND J. J. TIEMANN
General Electric Research and Development Center, Schenectady, New York
(Received 4 November 1966)

The strain-optical constants of Ge have been determined in the vicinity of the first indirect band gap 0.60–0.74 eV. The experiments were performed at room temperature and consisted of straining single crystals of Ge in an oscillatory manner and observing the amplitude modulation which was thereby impressed upon the transmitted beam. Single-crystal samples were used, allowing the full specification to be made. The results show both sharp structure and a relatively slowly varying background signal. The structure is discussed in terms of the strain-induced changes of the various threshold energies for indirect transitions expected on the basis of the deformation-potential model. The shape of the observed structure is in agreement with this simple model and the phonon energies are in excellent agreement with earlier determinations. The general features of the experimental results are explained in terms of indirect transitions taking place via the $\Gamma_{2'}$ intermediate state. A detailed calculation of the strain-optical constants made on the basis of the deformation-potential model indicates that direct transitions to $\Gamma_{2'}$ may also be important in this energy range.

I. INTRODUCTION

WHEN stress is applied to a solid, the optical properties of the material are altered. These changes may be measured and the results utilized to obtain information about the band structure and other fundamental properties of the solid. This paper describes a sensitive method for measuring these changes, which utilizes a periodically applied stress. The results of measurements made in the vicinity of the indirect optical-absorption edge of germanium are presented. A second paper will give the results of a similar measurement for silicon. A preliminary account of the Ge results has been presented previously.[1]

Periodic stress modulation of the reflectivity of semiconductors[2,3] and metals[2,4,5] has been shown to be a sensitive and useful technique. In principle, if these data are taken over a sufficiently wide energy range, they will yield, after a Kramers-Kronig analysis,[4,5] information concerning the changes in the optical constants of the solid caused by the strain. Piezoreflectivity, like the reflectivity itself, however, is quite insensitive to the relatively weak indirect optical transitions. The structure associated with the phonon-assisted transitions at the indirect edge of Ge, for example, is not observed in reflection. These weak processes must be observed in transmission. Piezotransmission measurements using static stress have recently been made[6] but because of lack of sensitivity, the phonon structure was not observed. The deformation potentials of silicon and germanium have recently been measured through the application of large static stresses and the use of the transmitted beam having a periodically oscillating wavelength.[7] The present experiment involves straining single-crystal samples of Ge in an oscillatory manner, thereby impressing some modulation upon the transmitted beam. This strain-modulated beam clearly shows the phonon and exciton

[1] W. E. Engeler, M. Garfinkel, and J. J. Tiemann, Phys. Rev. Letters **16**, 239 (1966).
[2] W. E. Engeler, H. Fritzsche, M. Garfinkel, and J. J. Tiemann, Phys. Rev. Letters **14**, 1069 (1965).
[3] G. W. Gobeli and E. O. Kane, Phys. Rev. Letters **15**, 142 (1965).
[4] W. E. Engeler, M. Garfinkel, J. J. Tiemann, and H. Fritzsche, in *Proceedings of the International Colloquium on Optical Properties and Electronic Structure of Metals and Alloys, Paris, 1965*, edited by F. Abeles (North-Holland Publishing Company, Amsterdam, 1966).
[5] M. Garfinkel, J. J. Tiemann, and W. E. Engeler, Phys. Rev. **148**, 695 (1966).
[6] E. Adler and E. Erlbach, Phys. Rev. Letters **16**, 87 (1966); **16**, 927 (1966).
[7] I. Balslev, Phys. Rev. **143**, 636 (1966).